NASA
Technical
Paper
2342

July 1984

Secondary Electron Emission Characteristics of Ion-Textured Copper and High-Purity Isotropic Graphite Surfaces

Arthur N. Curren
and Kenneth A. Jensen

NASA

NASA Technical Paper 2342

1984

Secondary Electron Emission Characteristics of Ion-Textured Copper and High-Purity Isotropic Graphite Surfaces

Arthur N. Curren
and Kenneth A. Jensen

Lewis Research Center
Cleveland, Ohio

National Aeronautics
and Space Administration

Scientific and Technical Information Branch

Summary

Experimentally determined values of true secondary electron emission and relative values of reflected primary electron yield for untreated and ion-textured oxygen-free, high-conductivity copper and untreated and ion-textured high-purity isotropic graphite surfaces are presented for a range of primary electron beam energies and beam impingement angles. This investigation was conducted to provide information that would improve the efficiency of multistage depressed collectors (MDC's) for microwave amplifier traveling-wave tubes in space communications and aircraft applications. For high efficiency, MDC electrode surfaces must have low secondary electron emission characteristics. Although copper is a commonly used material for MDC electrodes, it exhibits relatively high levels of secondary electron emission if its surface is not treated for emission control. Recent studies have demonstrated that high-purity isotropic graphite is a promising material for MDC electrodes, particularly with ion-textured surfaces. The materials were tested at primary electron beam energies of 200 to 2000 eV and at direct (0°) to near-grazing (85°) beam impingement angles. True secondary electron emission and relative reflected primary electron yield characteristics of the ion-textured surfaces were compared with each other and with those of untreated surfaces of the same materials. Both the untreated and ion-textured graphite surfaces and the ion-treated copper surface exhibited sharply reduced secondary electron emission characteristics relative to those of untreated copper. The ion-textured graphite surface yielded the lowest emission levels.

Introduction

An important consideration in the development of high-efficiency microwave amplifier traveling-wave tubes (TWT's) for space communications and aircraft applications is the achievement of high collector efficiency. The invention and development of the multistage depressed collector (MDC) for these tubes (ref. 1) has been a major contribution to this effort. Among the significant factors in maximizing MDC efficiency is the use of electrode materials with low secondary electron emission characteristics. Specifically, to usefully recover the maximum kinetic energy from the spent electron beam after it has passed through the TWT's radio-frequency interaction section and entered the MDC, the electrodes must have low secondary electron emission characteristics (ref. 2) so that the electrons are not excessively reflected or reemitted from the surfaces.

Ion texturing of some candidate MDC electrode surfaces significantly reduces secondary electron emission characteristics relative to the untreated surfaces of the same materials (refs. 3 to 5). An ion-textured (pyrolytic graphite) MDC electrode set was tested with a full-scale TWT at the NASA Lewis Research Center (ref. 6). The MDC and TWT efficiencies were higher than those of the same TWT tested with untreated pyrolytic graphite or untreated copper MDC electrode sets. The ion-textured surfaces examined in the present study included oxygen-free, high-conductivity (OFHC) copper and high-purity isotropic graphite. The true secondary electron emission and relative reflected primary electron yield characteristics of these surfaces were compared with each other and with those characteristics of the same materials with untreated surfaces.

To properly assess the effectiveness of proposed MDC electrode materials, we must have good knowledge of their secondary electron emission characteristics over a representative range of electron beam impingement angles and over a wide range of primary electron beam energy levels. This report is intended to contribute to that knowledge for the materials investigated.

Background Information

TWT and MDC Considerations

High-efficiency microwave amplifier TWT's use MDC's. The magnetic field that confines the electron beam in the radiofrequency interaction section of the TWT is removed at the MDC entry port. From this point the beam diverges, and the electrons are slowed by a retarding electrical field and collected selectively by electron energies, with relatively small losses. The MDC efficiency is directly influenced by the ability of the electrodes to absorb and retain the impinging electrons. To attain the highest efficiency, the electrodes must have a low secondary electron emission ratio, or ratio of

reemitted electrons to impinging electrons. Secondary electron emission as an MDC loss mechanism is discussed in references 3 and 5.

Materials Investigated

OFHC copper.—Oxygen-free, high-conductivity (OFHC) copper is widely used for MDC electrodes. Although this material has high thermal conductivity, is relatively easy to machine, and has well-developed fabrication and brazing procedures, it has relatively high secondary electron emission characteristics in a smooth or moderately abraded surface condition. Topical treatments such as sputter-applied titanium carbide have been used with copper to moderately reduce the emission characteristics. Experiments conducted at the NASA Lewis Research Center have indicated significant reductions in the secondary emission characteristics of copper when the surface is appropriately ion textured. The OFHC copper samples investigated in this study were ion textured at Lewis by a method described later.

High-purity isotropic graphite.—The graphite used in this study was characterized by high purity, adequate physical strength for the MDC electrode application, and excellent machinability. Although other suitable premium commercial grades of graphite are available from several domestic producers, the graphite used in this study was purchased from Poco Graphite, Inc., a Union Oil Company subsidiary, 1601 South State Street, Decatur, Texas 76234. The grade of Poco Graphite selected with DFP-2, which the manufacturer's literature describes as having negligible variations in property values with direction of measurement.

Table I presents for comparison some selected properties of the OFHC copper (from ref. 7) and the isotropic graphite (from ref. 8) used in this study. The isotropic graphite has a definite density advantage over the OFHC copper, although its thermal conductivity is considerably lower. Total normal thermal emissivity, an important consideration in MDC thermal control, is much higher for the isotropic graphite than for the OFHC copper. Very importantly, the coefficient of thermal expansion for the isotropic graphite is very near to those for typical ceramics (Al_2O_3, ZrO_2, or BeO) (ref. 7) to which electrodes are customarily brazed in MDC structures. This property characteristic suggests fewer brazing problems for the isotropic graphite electrode-to-ceramic interface. Where greater differences in thermal expansion coefficients occur, such as in OFHC copper electrode-to-ceramic interfaces, brazing procedures require special consideration.

Again as with OFHC copper, experiments conducted at the NASA Lewis Research Center have indicated sharply reduced secondary electron emission characteristics for appropriately ion-textured isotropic graphite relative to those for the untreated surface. The isotropic graphite samples investigated in this study were also ion textured at Lewis by a method described in the following section.

Experimental Procedures

Ion Texturing

A schematic diagram of the ion-texturing apparatus used in this investigation (fig. 1) is described, along with its operating procedures, in reference 5. Briefly, the samples tested were positioned in the sample receptacle shown in the figure and were subjected to argon ion

TABLE I.—SOME SELECTED PROPERTIES OF OFHC COPPER AND HIGH-PURITY ISOTROPIC GRAPHITE

Property	OFHC copper	High-purity isotropic graphite
Density at RT[a], g/cm^3	8.94	1.84
Melting or sublimation temperature, °C	1083	3350
Tensile strength at RT, Pa (psi)	1.93×10^8 (28 000)	5.52×10^7 (8000)
Compressive strength at RT, Pa (psi)	----------	1.31×10^8 (19 000)
Yield strength at RT (for 0.5-percent extension under load), Pa (psi)	5.45×10^7 (7900)	----------
Coefficient of thermal expansion at RT, cm/cm/°C	16.5×10^{-6}	7.7×10^{-6}
Thermal conductivity at RT, cal/cm^2/cm/sec/°C	0.934	0.289
Specific heat at RT, cal/g/°C	0.092	<0.2
Total normal thermal emissivity at RT	0.023	0.80 - 0.85
Modulus of elasticity at RT, Pa (psi)	1.10×10^{11} (16×10^6)	1.10×10^{11} (1.6×10^6)
Average pore size, μm	----------	0.4
Average purity, ppm-total ash	----------	5
Porosity, percent	----------	19

[a]RT indicates room temperature.

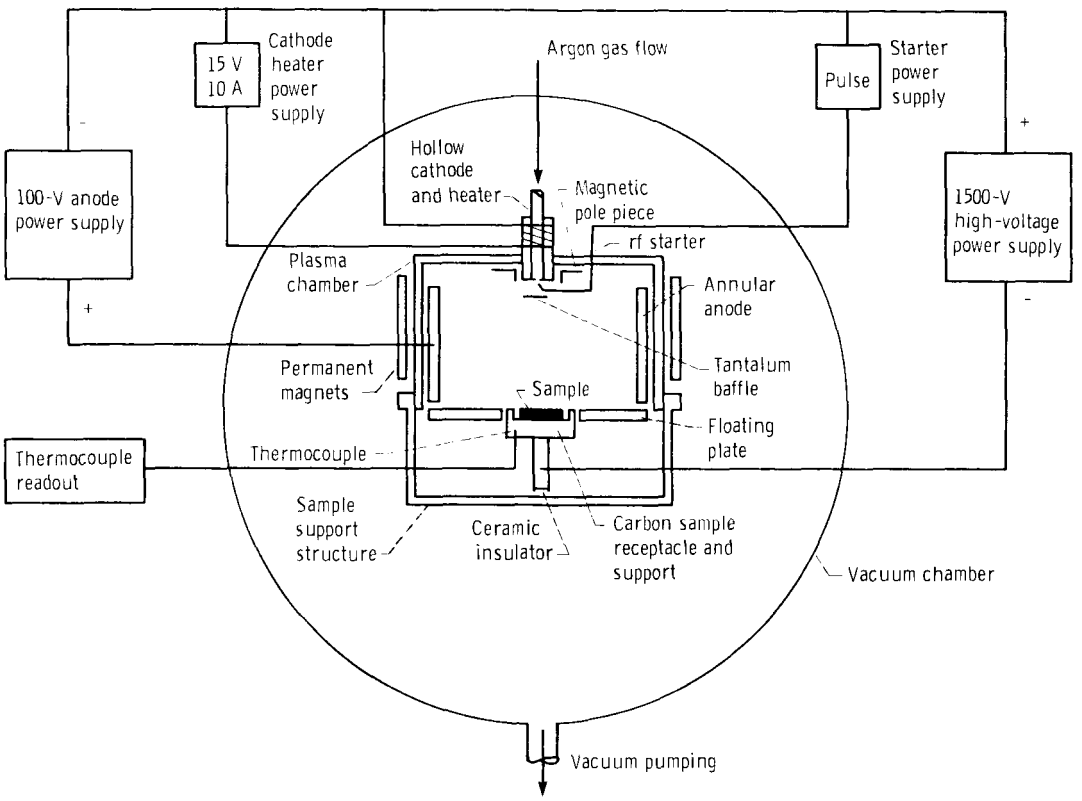

Figure 1.—Schematic of ion-texturing apparatus.

bombardment in a low-pressure (approx 2.66 mPa; 2×10^{-5} torr) environment. The accelerating potential difference between the plasma and the sample was an operating variable, along with the argon gas flow rate, the sample surface current density, and the duration of ion bombardment. The samples were disks approximately 2.1 cm (0.828 in.) in diameter by 0.15 cm (0.060 in.) thick. The OFHC copper disk surfaces were cleaned by gentle abrasion with extremely fine sanding cloth. Then, immediately before they were textured, both the OFHC copper samples and the isotropic graphite samples were cleaned by successively wiping them with clean acetone and high-purity ethyl alcohol on a clean lint-free cloth or absorbent paper.

The OFHC copper and isotropic graphite samples are shown positioned in the sample support receptacle before they were installed in the ion-texturing apparatus (fig. 2). The OFHC copper sample (fig. 2(a)) is surrounded by a narrow tantalum skirt located a short distance (about 0.95 cm; 0.375 in.) above its surface and sloping outward at a 45° angle. OFHC copper does not spontaneously form the desired surface structure (to be described subsequently) under ion bombardment. However, a relatively higher melting-point material such as tantalum arranged approximately in the position shown relative to the material to be textured "seeds" the copper surface (ref. 9) and causes ion texturing of the copper to occur. Placement of the seeding material is important for uniform texturing (and consequently uniformly low secondary electron emission properties) over the copper surface. Some experimentation with the placement of the seeding material may be required to produce uniform texturing over the surface of some OFHC copper configurations.

The isotropic graphite sample support arrangement (fig. 2(b)) is very simple since this and some other graphite forms texture spontaneously under ion bombardment with no special arrangement of other materials required (refs. 4 to 6).

Secondary Electron Emission Evaluation

The facilities and procedures used to evaluate the secondary electron emission characteristics of the OFHC copper and isotropic graphite samples investigated in this study are described in detail in reference 5. Briefly, the samples were attached to a micromanipulator-mounted support fixture and installed in an ultra-high-vacuum vessel equipped with a scanning Auger spectrometer cylindrical mirror analyzer (CMA) that had an integral electron gun, a residual gas analyzer (RGA), vacuum feedthrough fittings, and other associated equipment. A filament heater-reflector system and a thermocouple were incorporated into the sample-holding fixture for sample

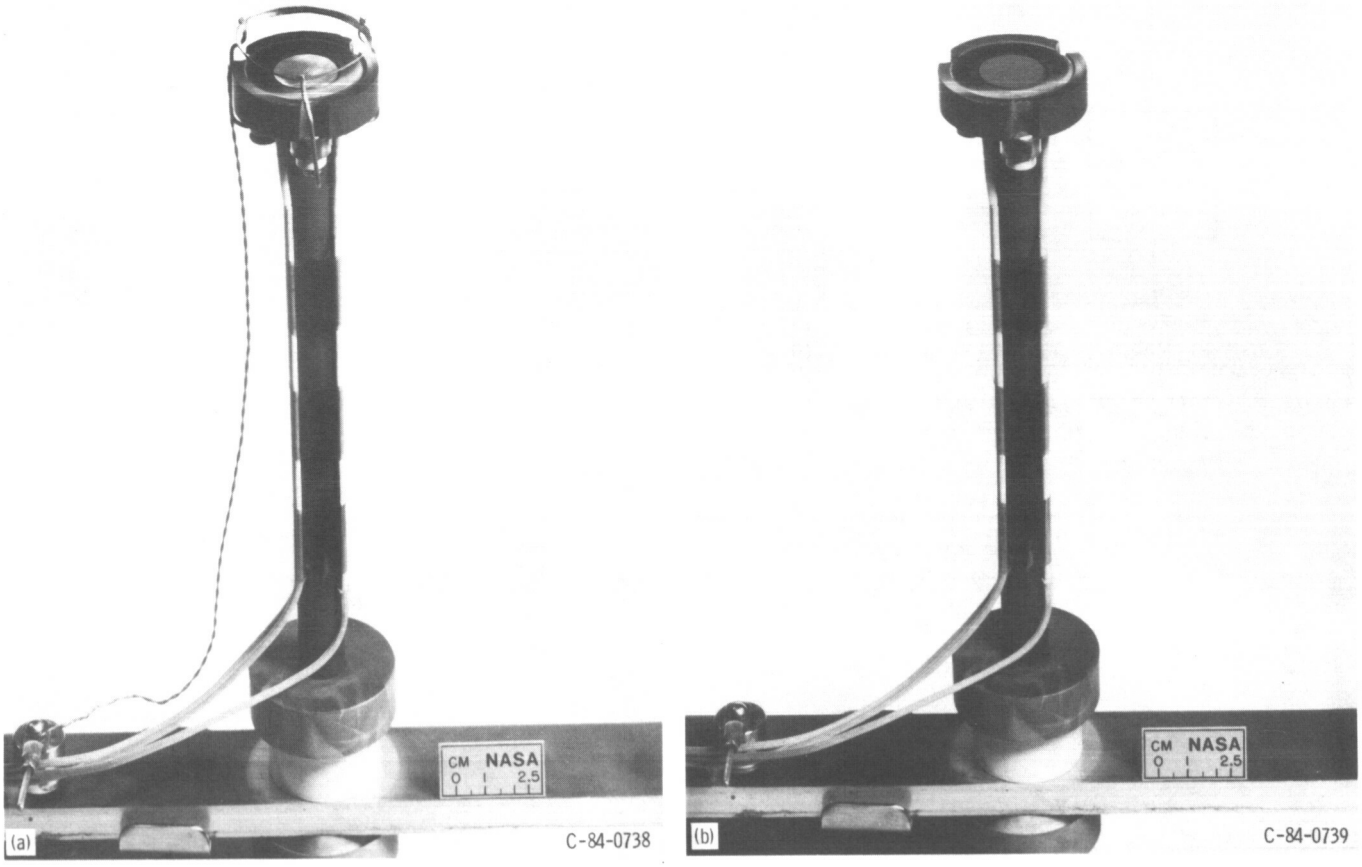

(a) OFHC copper sample. Note tantalum skirt surrounding sample position.
(b) Isotropic graphite sample.

Figure 2.—Sample supports and receptacles with samples in position before installation in ion-texturing apparatus.

degassing and temperature monitoring. The vacuum chamber was evacuated to a pressure of 13.3 nPa (1×10^{-10} torr) or less for testing. During the pumpdown the entire vacuum chamber was heated to about 250° C for 16 hours to degas the system. After that procedure the sample was heated by filament radiation and electron bombardment to about 500° C for 3 to 4 hours to further degas the sample and simulate the anticipated "bakeout" temperature to which an MDC assembly on a TWT would be subjected. Along with the secondary electron emission measurements, Auger spectroscopic examinations were conducted to determine the chemical compositions of the sample surfaces. These examinations and measurements are discussed in the section Experimental Results.

The bottom half of each sample disk included in this investigation was coated with soot to provide a control surface. The affected areas of the ion-textured samples were smoothed to return the surfaces as nearly as possible to their untreated condition before the soot coating was applied. During the evaluation of the sample surfaces for secondary electron emission characteristics, tests were routinely performed at two or more locations on each half of the disk surface. This procedure helped to ensure the validity of the data since the well-known and readily repeatable very low secondary electron emission characteristics of soot provided a "standard" that would immediately indicate errors in procedure or instrument function should they occur.

The surfaces studied in this investigation were evaluated for true secondary electron emission and reflected primary electron yield characteristics at 11 primary electron beam energy levels from 200 to 2000 eV for each of eight beam impingement angles from 0° (directly impinging) to 85° (near grazing). For each angle the electron gun was focused to produce a spot diameter at the sample of about 10 μm. Tests at identical conditions were routinely repeated and yielded repeatable results (within limits of measurement) in every instance. Scanning electron microscope examinations after lengthy periods of testing revealed no observable surface damage from electron beam impingement for any of the surfaces.

True secondary electron emission.—In true secondary electron emission, electrons undergo inelastic collisions at or near a solid surface that is undergoing electron bombardment and are emitted from that surface with

energies of the order of a few tens of electron volts. A sample-biasing method that is described in detail in reference 5 was employed to determine the true secondary electron emission characteristics of the surfaces investigated in this study. Briefly, with the electron beam focused on the sample surface with a given beam energy level, the measured sample-to-ground current was taken to be the total beam current minus the secondarily emitted current. When an appropriate positive bias voltage (in this case, 90 V) was then applied to the sample, the true secondary electrons were retained by the sample and the resulting measured sample-to-ground current was taken to be the total beam current. The true secondary electron emission ratio δ, or ratio of true secondarily emitted electrons to primary electrons, was calculated by the expression

$$\delta = \frac{I_b - (I_b - I_s)}{I_b}$$

where

$I_b - I_s$ beam current minus secondarily emitted current (0.05 to 3.5 μA in this study)

I_b beam current (0.27 to 7.4 μA in this study)

Reflected primary electron yield.—In reflected primary electron yield, electrons experience elastic collisions at a solid surface that is undergoing electron bombardment and are reflected from that surface with energies at or very nearly at the primary electron beam energy level. The method for evaluating the reflected primary electron yield for the surfaces studied in this investigation was adapted from that used in reference 3. The Auger CMA was used to characterize the reflected primary yield at each primary electron beam energy level investigated. The quantity used as a measure of the relative values of reflected primary yields from different surfaces at a given primary electron beam energy and impingement angle was the "reflected primary electron yield index." This is the ratio of the amplitude of the elastic energy peak for a given surface and a given primary electron energy to the amplitude of the elastic energy peak for the control soot surface at the same beam impingement angle and a primary electron beam energy of 1000 eV. The reflected primary electron yield index π is given by

$$\pi_{eV'} = \frac{D_{sample}}{D_{control}}$$

where

D_{sample} elastic curve amplitude for sample surface at primary electron beam energy eV′

$D_{control}$ elastic curve amplitude for soot control surface at 1000-eV primary electron beam energy

As has been stated, soot was selected for the control surface, as it was in reference 3, because of its known extremely low secondary electron emission characteristics and its ability to be readily reproduced. Although this method does not determine the absolute value of the reflected primary electron yield, it serves the important purpose of permitting comparison of this property for different surfaces.

Note that the primary electron yield that was measured and that is reported in this study was based only on those electrons that were reflected directly at or very nearly directly at the Auger CMA, which contained the primary electron source. This therefore was the most important direction of emission from the standpoint of MDC efficiency.

Experimental Results

Surfaces Investigated

Scanning electron microscope photomicrographs of the four surfaces studied in this investigation are presented in figure 3. All of the photographs were taken at the same magnification for ease of comparison. The untreated but lightly sanded and cleaned OFHC copper surface (fig. 3(a)) is shown just before it was installed in the ion-texturing apparatus or the secondary electron emission testing facility. This surface had no major projections, but high magnification revealed numerous very shallow scratch-like depressions from the light sanding procedure. This degree of surface smoothness is probably representative of the OFHC copper MDC electrodes in practical application. The surface characteristics shown in figure 3(b) were created when an OFHC copper surface (fig. 3(a)) was ion textured by using the parameters indicated. The dense random array of projections extended perpendicularly from the surface to an average uniform height of about 10 μm, with an average spacing of about 5 μm. The projections had nearly vertical sides and were relatively blunt ended; some appeared to be hollow. A cleaned, untreated isotropic graphite surface is shown (fig. 3(c)) just before ion texturing or secondary electron emission testing. This surface had been dry machined but was not sanded or otherwise abraded or polished. It had no major projecting features but was obviously quite porous. When the untreated isotropic graphite surface was ion textured according to the parameters indicated, the surface features shown in figure 3(d) developed. This surface displayed a closely arrayed pattern of perpendicular conical spires averaging 5 μm in height and 3 μm in spacing. The spire projections on this surface were not as uniform in height as were the blunt

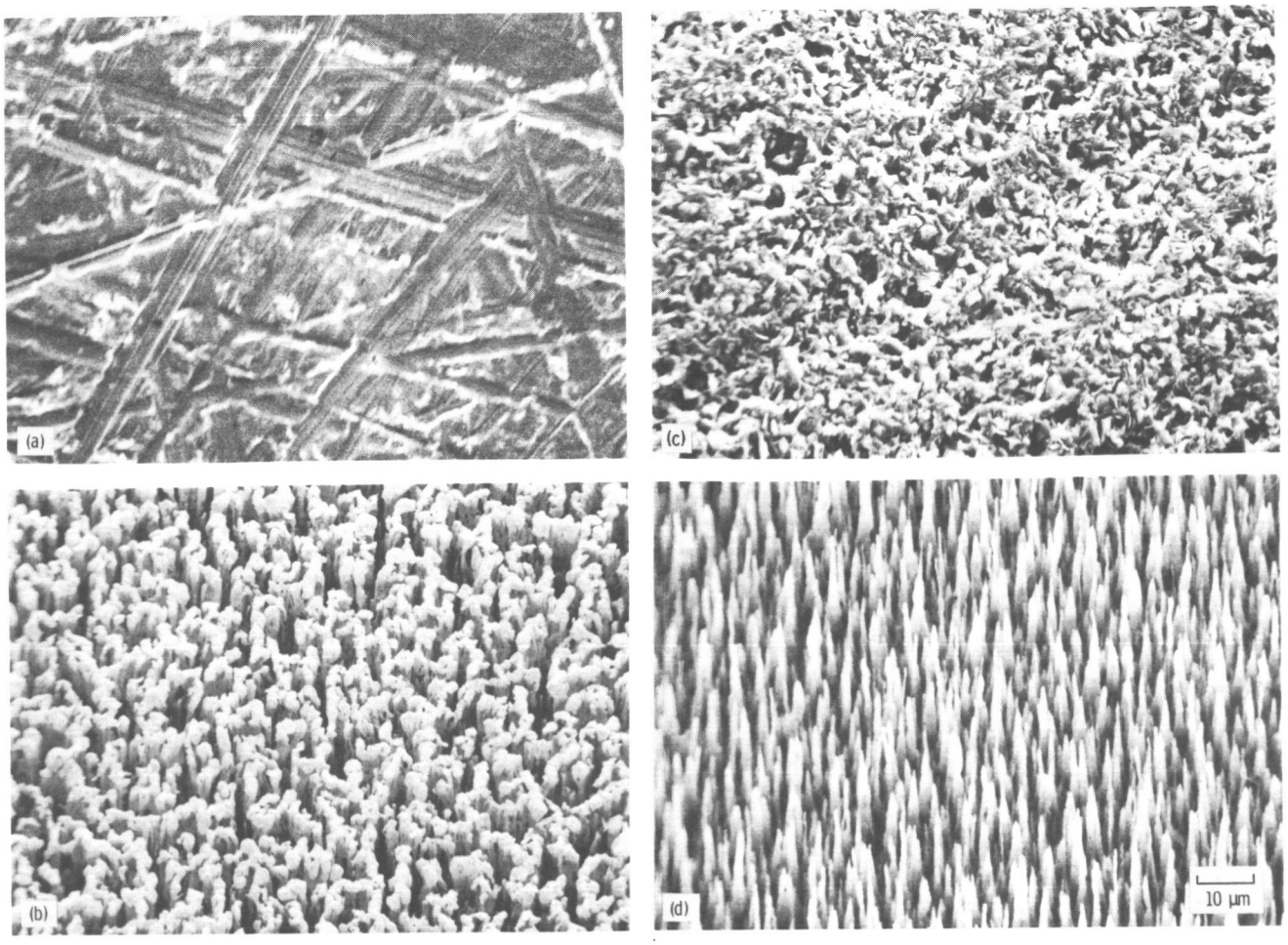

(a) Untreated OFHC copper surface.

(b) Ion-textured OFHC copper surface. Texturing parameters: surface current density, 5 mA/cm^2; target or "seed" material, tantalum; texturing period, 3 hr; temperature (sample receptacle average), 420° C.

(c) Untreated isotropic graphite surface.

(d) Ion-textured isotropic graphite surface. Texturing parameters: surface current density, 3 mA/cm^2; texturing period, 4 hr; temperature (sample receptacle average), 500° C.

Figure 3.—Electron microscope photographs of sample surfaces examined for secondary electron emission characteristics. Angle with surface, 30°. Common texturing parameters; accelerating potential, 1500 V dc; argon flow rate, 60 std cm^3/min; vacuum chamber pressure, ~2.7 mPa (2×10^5 torr).

projections on the ion-textured OFHC copper surface. Many of the spires on the ion-textured isotropic graphite surface appeared to be immature or not fully developed.

The physical appearances of the materials investigated in this study were changed markedly by the ion texturing process. The contrast in appearance between untreated and ion-textured OFHC copper and untreated and ion-textured isotropic graphite is shown in figure 4. In each case, the dense array of microscopic projections gave the ion-textured surfaces a much darker appearance than the untreated surfaces. This characteristic of the ion-textured surfaces also suggests a significant increase in thermal emissivity relative to the untreated surfaces.

The ion-texturing procedures used in this investigation were not necessarily those that produce "optimum" surfaces for secondary electron emission suppression. Rather, the procedures were those that were being studied when this investigation began and that have been shown to result in surfaces whose secondary electron emission characteristics are much lower than those of the respective untreated surfaces.

Surface Auger Spectroscopic Examinations

Auger spectroscopic examinations of each of the sample surfaces investigated were conducted immediately before secondary electron emission testing. The Auger spectra for the ion-textured OFHC copper and ion-textured isotropic graphite surfaces are presented in figure 5. The presence of the "seeding" material, tantalum, is indicated by a prominent peak pattern on the curve for ion-textured OFHC copper. It is this covering

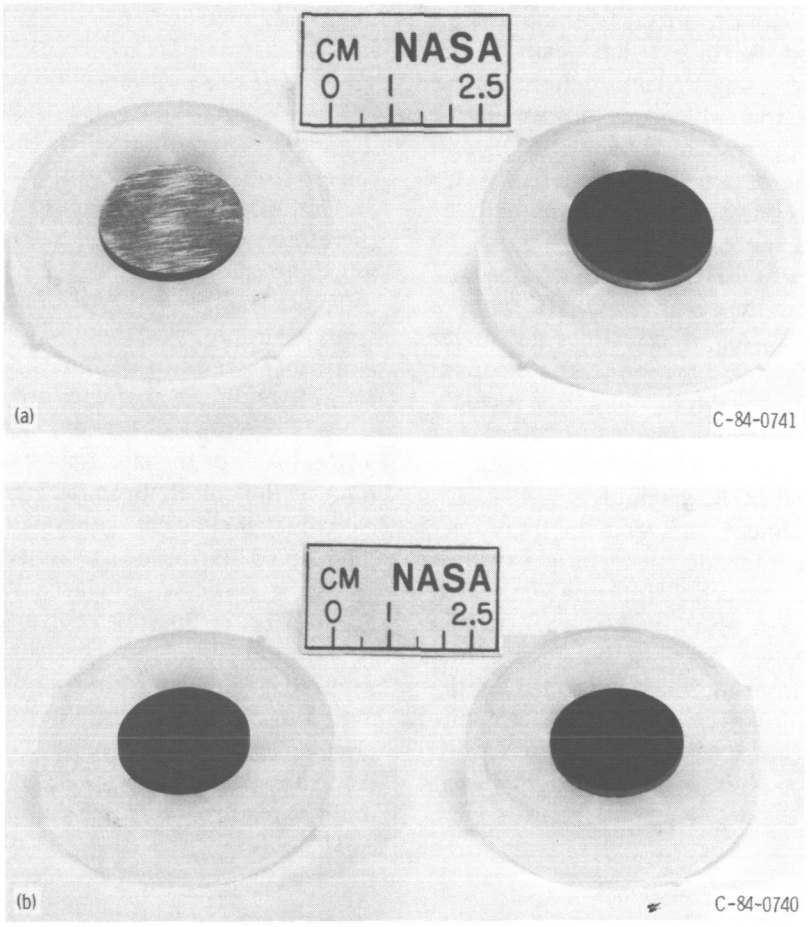

(a) OFHC copper samples.
(b) Isotropic graphite samples.

Figure 4.—Contrast in appearance of untreated (left) and ion-textured (right) samples. Samples are shown in storage containers.

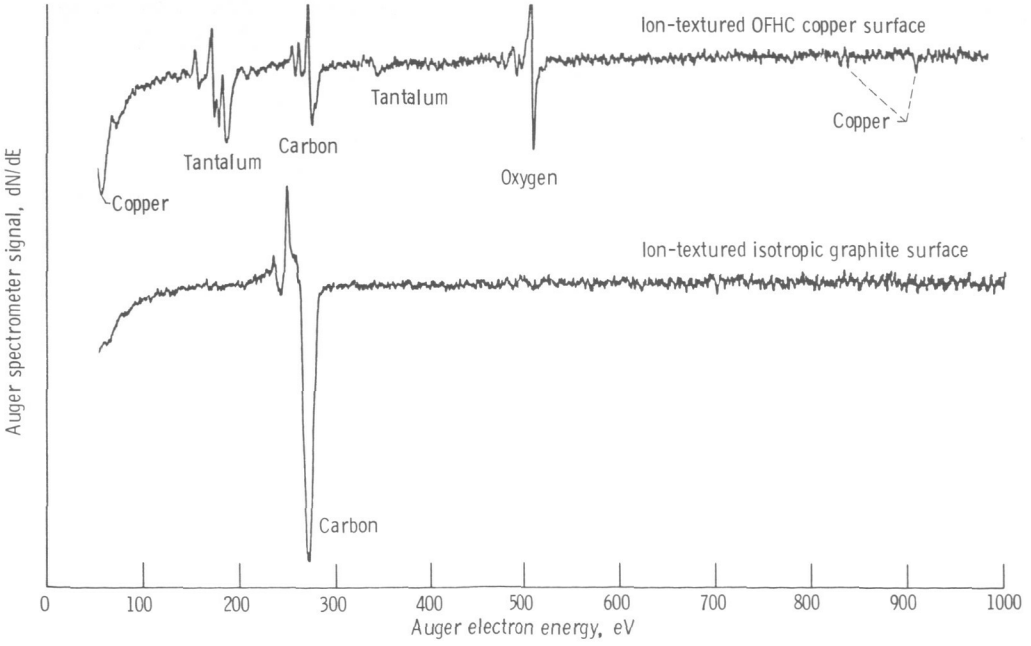

Figure 5.—Postbakeout Auger spectra for ion-textured OFHC copper and ion-textured isotropic graphite surfaces.

layer of tantalum, along with the effects of the emission-attenuating ion-textured surface, that causes the amplitude of the copper Auger peak pattern to be significantly smaller than that which would normally be expected for a clean copper surface. The carbon and oxygen indicated as being present are tenacious surface contaminants that resist removal by the bakeout methods used in this study and were observed on both the untreated and ion-textured OFHC copper surfaces. The Auger spectrum for the ion-textured OFHC copper surface shown in figure 5 strongly resembles the Auger spectrum presented in reference 3 for ion-textured copper after degassing (at 600° C) and ion cleaning. The surfaces investigated in this study were not ion cleaned, since that procedure would not be representative of the treatment of electrodes in a practical MDC assembly.

Carbon is the only element indicated on the Auger spectrum shown in figure 5 for the ion-textured isotropic graphite surface. Auger spectra for the untreated isotropic graphite surfaces examined were virtually identical to the curve shown. Some indications of the presence of argon (the texturing ion) were noted on the Auger spectra for some ion-textured isotropic graphite surfaces taken before the 500° C bakeout described elsewhere in this report, but argon apparently was entirely removed during the degassing procedure.

Secondary Electron Emission Measurements

The experimental results presented in this report are not average or mean values for several "identical" test conditions but are specific values for one particular test series for each surface examined that were judged to be typical for that surface. A relatively large number of test series were performed during the investigation to form the basis of that judgment. Furthermore, specific test conditions were repeated routinely for each surface at different locations on the surface to assure the validity of the data recorded. Scanning electron microscope examinations were conducted for each surface to assure uniform conditions and to reduce the possibility of inadvertently selecting an unusual or atypical location for testing.

True secondary electron emission.—For each of the four surfaces studied in this investigation, the true secondary electron emission ratio increased with electron beam impingement angle at all points over the primary electron energy range examined. This is illustrated in figures 6(a), 7(a), 8(a), and 9(a), where the emission ratio is presented as a function of primary electron energy for each of the electron beam impingement angles examined.

The reasons for the observed increase in true secondary electron emission ratio with electron beam impingement angle are probably different for the two general types of surface examined. As the electron beam impingement angle was increased for the two relatively smooth surfaces, untreated OFHC copper and untreated isotropic graphite (figs. 3(a) and 6(a), and 3(c) and 8(a), respectively), the impringing electrons penetrated to decreasing distances below the level of the surfaces. Consequently the electrons that were involved in the inelastic collisions had a shorter distance to travel to escape the surfaces and therefore escaped in increasing numbers as the beam angle increased.

The second general type of surface investigated in this study, the ion-textured OFHC copper and ion-textured isotropic graphite samples (figs. 3(b) and 3(d), respectively) were characterized by closely arrayed spires or peaks. With a direct (0°) electron beam impingement angle, many of the electrons struck the spire walls or the base of the spires. Because many of the true secondary electrons that were generated then were repeatedly intercepted by the nearby spire walls, the net emission from the projected surface area was reduced. As the electron beam impingement angle was increased, beam penetration into the complex surface structure was reduced. The resulting lower secondary electron "trapping" effect permitted the net true secondary electron emission to increase. The increase is illustrated in figures 7(a) and 9(a) for the ion-textured OFHC copper and ion-textured isotropic graphite surfaces, respectively.

The ion-textured isotropic graphite clearly displayed the lowest true secondary electron emission ratio at all electron beam energies and beam impingement angles examined of all of the material surfaces included in this investigation. Comparing the true secondary electron emission ratio characteristics of the ion-textured isotropic graphite with those of the "ideal" soot surface reported in reference 5 indicated lower emission ratio levels for the ion-textured isotropic graphite at all beam impingement angles for electron beam energy levels above about 750 eV and at angles less than about 60° for energies less than 750 eV. Furthermore, the true secondary electron emission ratio characteristics of the ion-textured isotropic graphite were quite similar to those of the ion-textured pyrolytic graphite surfaces reported in reference 5.

Reflected primary electron yield.—Curves presenting the reflected primary electron yield index π, which is the primary yield relative to that of soot at 1000-eV primary electron beam energy, for the surfaces investigated in this study appear in figures 6(b), 7(b), 8(b), and 9(b). The two relatively smooth surfaces, untreated OFHC copper and untreated isotropic graphite (figs. 3(a) and 6(b), and 3(c) and 8(b), respectively) exhibited generally decreasing levels of reflected primary electron yield index with beam impingement angle over the primary electron beam energy range investigated. For these surfaces, impinging electrons that experienced elastic collisions reflected increasingly in directions away from the Auger CMA as the beam impingement angle was increased. This resulted

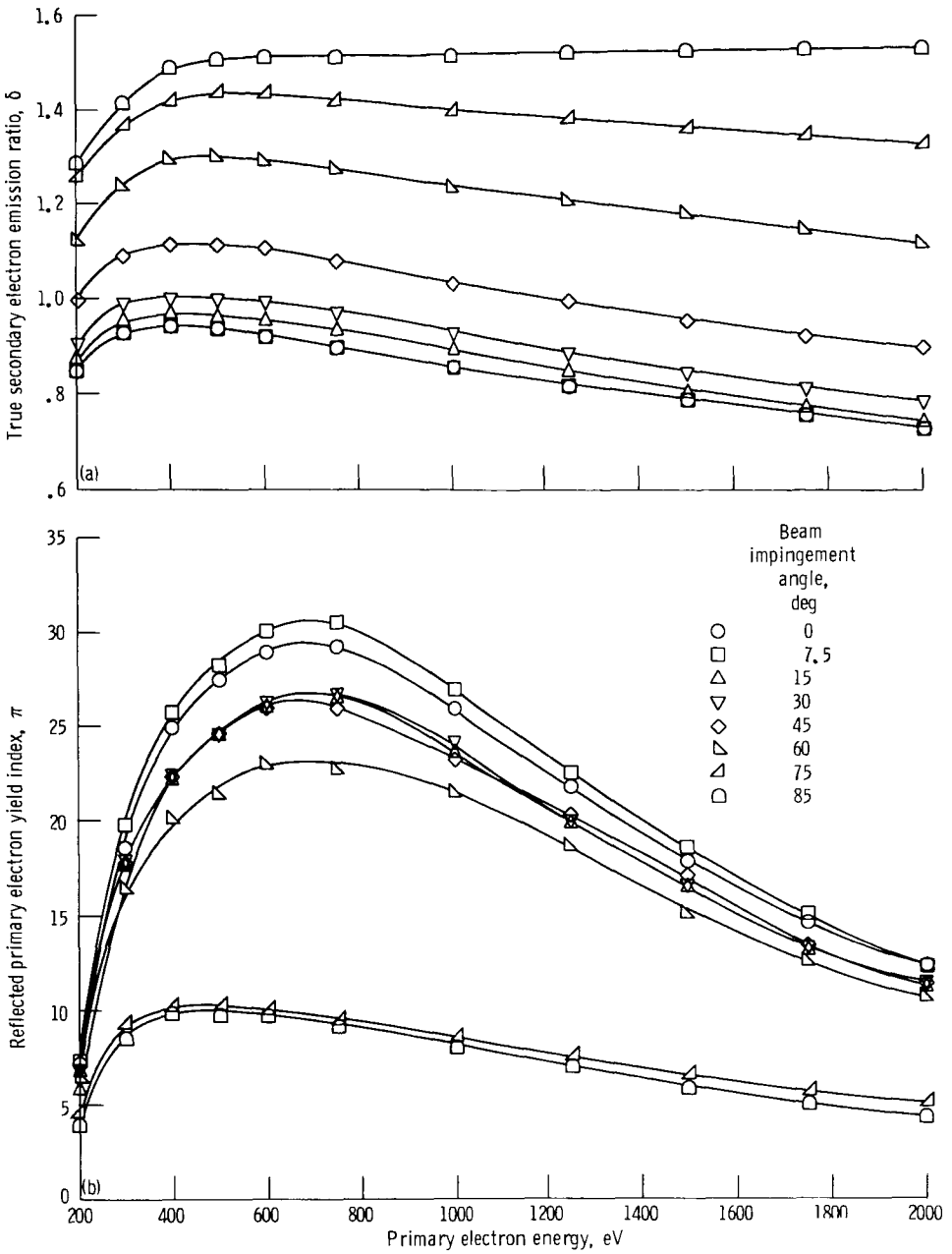

(a) True secondary electron emission ratio.
(b) Reflected primary electron yield index.

Figure 6.—Characteristics of untreated OFHC copper surface as function of primary electron energy.

in increasingly smaller measurements of reflected primary electron yield. Conversely the other two surfaces studied, ion-textured OFHC copper and ion-textured isotropic graphite (figs. 3(b) and 7(b), and 3(d) and 9(b), respectively) displayed increasing levels of reflected primary electron yield index with electron beam impingement angle over the same energy range. As the electron beam impingement angle was increased for these surfaces, much of the area on which the beam impinged (the sides of the spires) was rotated so that it increasingly moved toward directly facing the Auger CMA. This resulted in the observed increase in measured reflected primary electron yield as the beam impingement angle was increased.

Although the ion-textured isotropic graphite exhibited lower measured reflected primary electron yield than the untreated isotropic graphite at all points examined, a comparison of the reflected yield characteristics for untreated and ion-textured OFHC copper surfaces is more complex. For beam impingement angles to about

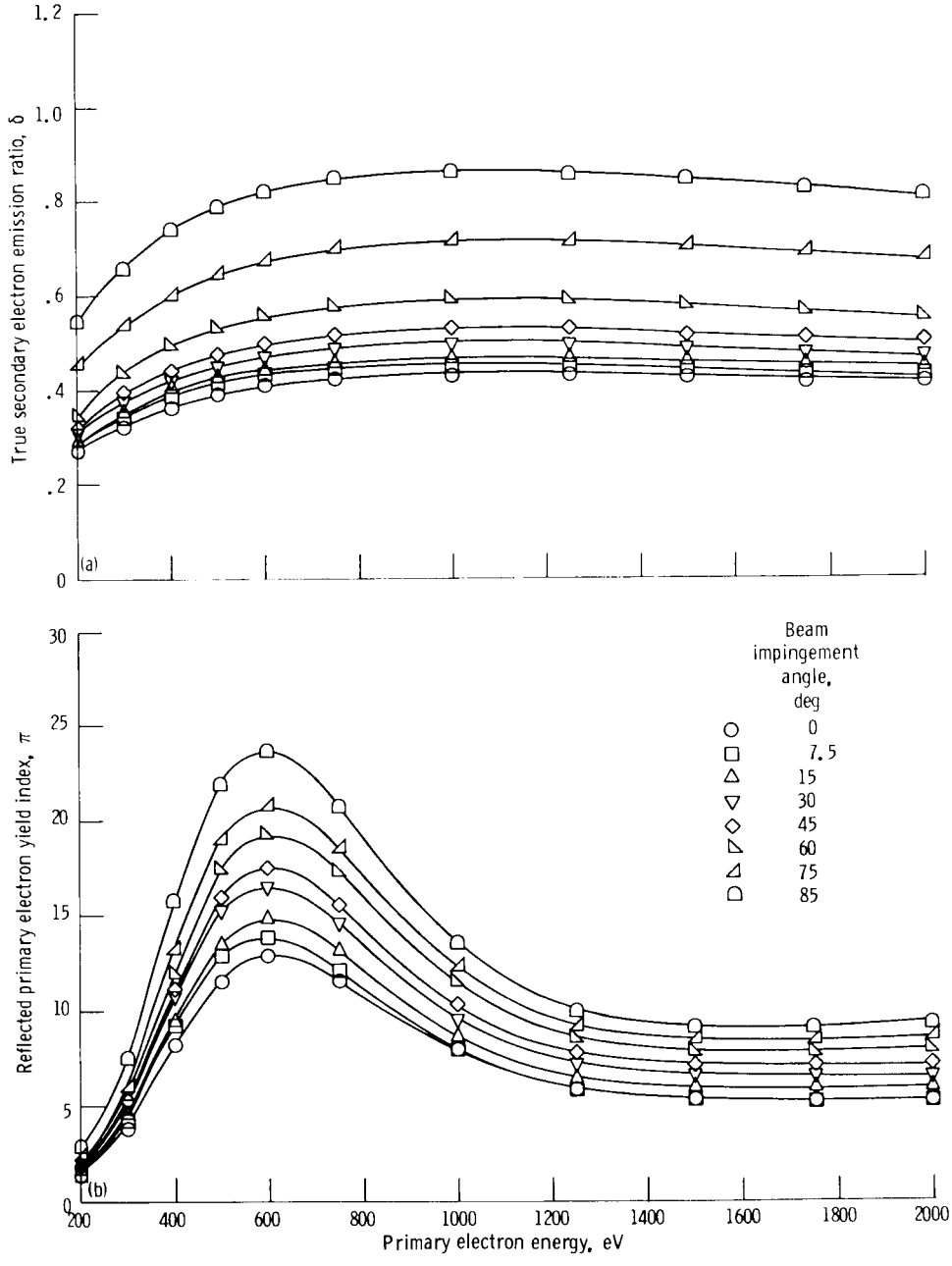

(a) True secondary electron emission ratio.
(b) Reflected primary electron yield index.

Figure 7.—Characteristics of ion-textured OFHC copper surface as function of primary electron energy.

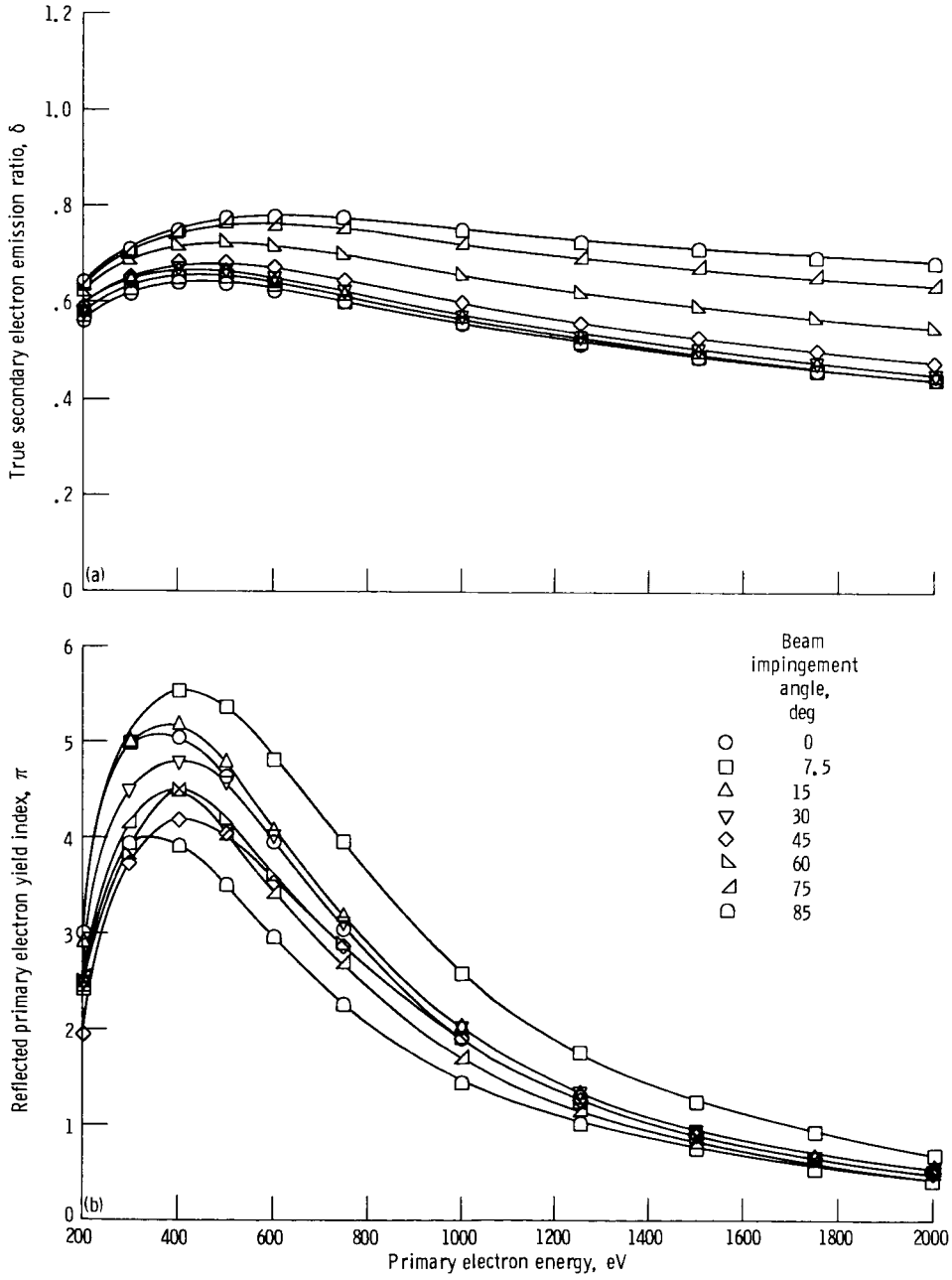

(a) True secondary electron emission ratio.
(b) Reflected primary electron yield index.

Figure 8.—Characteristics of untreated isotropic graphite surface as function of primary electron energy.

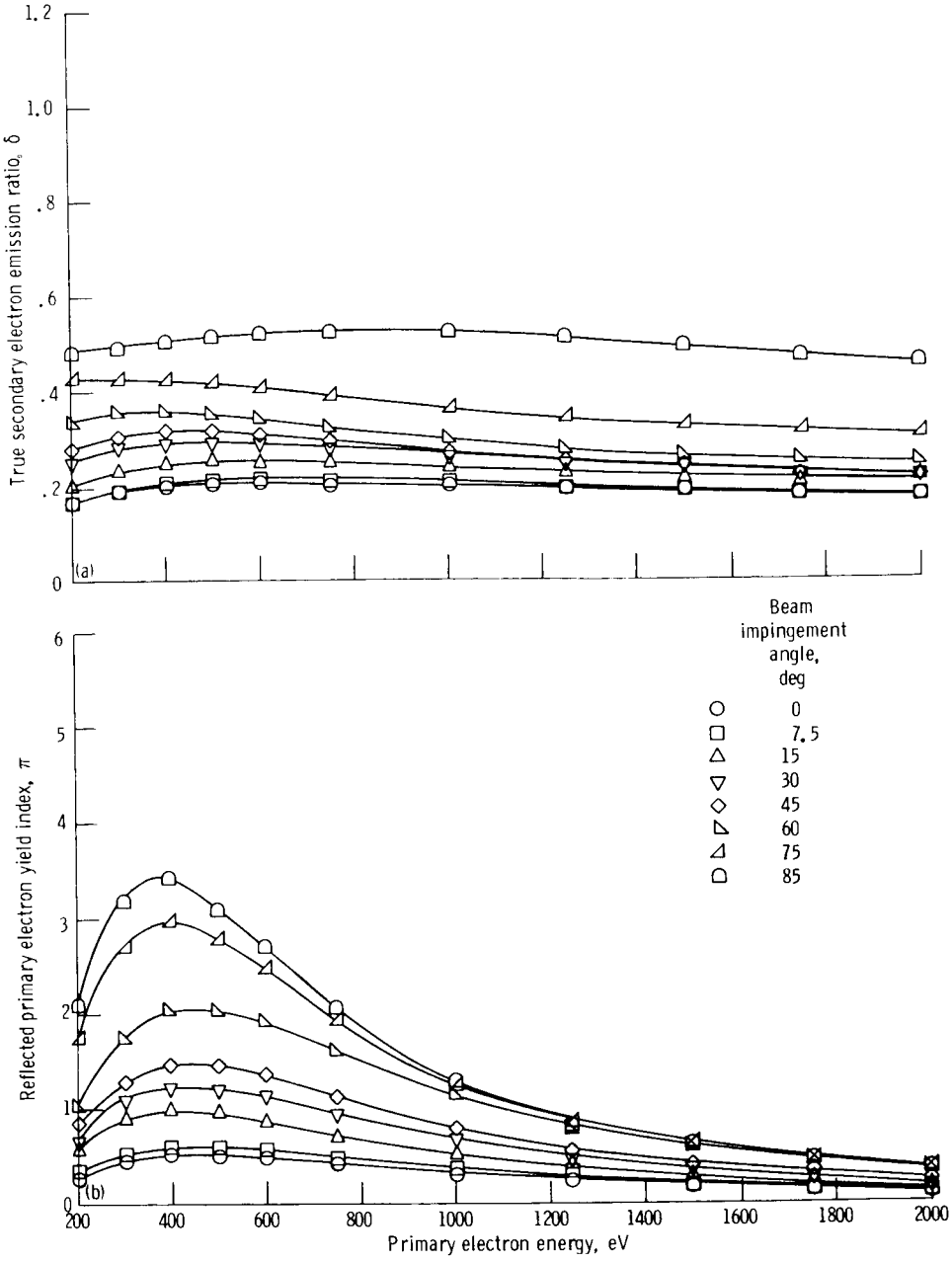

(a) True secondary electron emission ratio.
(b) Reflected primary electron yield index.

Figure 9.—Characteristics of ion-textured isotropic graphite surface as function of primary electron energy.

60° and over the entire electron beam energy range studied, the ion-textured OFHC copper surface displayed the lower yield levels. At beam impingement angles greater than 60°, however, the untreated OFHC copper surface exhibited the lower measured reflected primary yield.

Again as with the true secondary electron emission measurements, the ion-textured isotropic graphite surface displayed the lowest level of measured reflected primary electron yield of the surfaces examined in this study. Furthermore, the low measured yield levels for this surface were comparable to, and in some cases lower than, the levels for the ion-textured pyrolytic graphite surfaces reported in reference 5.

Conclusions

Untreated and ion-textured OFHC copper and high-purity isotropic graphite surfaces were experimentally investigated to determine their true secondary electron emission and relative reflected primary electron yield characteristics. The surfaces were tested over a range of primary electron beam energies from 200 to 2000 eV and at beam impingement angles from direct (0°) to near grazing (85°). The purpose of the investigation was to assess the use of ion-textured OFHC copper and untreated and ion-textured isotropic graphite as materials for electrodes in multistage depressed collectors (MDC's) for high-efficiency microwave amplifier traveling-wave tubes (TWT's) in space communications and aircraft applications. To attain high efficiency in MDC's, the electrode surfaces must have low secondary electron emission characteristics. Untreated OFHC copper was used as a basis of comparison for the other surfaces examined because it is currently in wide use as an MDC electrode material.

The untreated and ion-textured isotropic graphite surfaces displayed significantly lower true secondary electron emission and reflected primary electron yield index levels than untreated OFHC copper over the primary electron beam energy and beam impingement angle ranges tested. Ion-textured OFHC copper also exhibited much lower true secondary electron emission than untreated OFHC copper over the ranges tested. However, at electron beam angles greater than about 60°, the reflected primary electron yield index of the untreated OFHC copper was somewhat lower.

The results of this investigation indicate that any one of the other three surfaces studied would perform more effectively, from the standpoint of secondary electron emission characteristics in the range of conditions considered, in the MDC electrode application than untreated OFHC copper. Of those three, however, the high-purity isotropic graphite surface clearly provided the best potential to improve MDC and therefore TWT overall efficiency.

Lewis Research Center
National Aeronautics and Space Administration
Cleveland, Ohio, April 27, 1984

References

1. Kosmahl, H. G.: A Novel, Axisymmetric, Electrostatic Collector for Linear Beam Microwave Tubes. NASA TN D-6093, 1971.
2. Kosmahl, H. G.; and Ramins, P.: Small-Size 81- to 83.5-Percent Efficient 2- and 4-Stage Depressed Collectors for Octave-Bandwidth High-Performance TWT's. IEEE Trans. Electron. Devices, vol. ED-24, Jan. 1977, pp. 36-44.
3. Forman, R.: Secondary-Electron-Emission Properties of Conducting Surfaces with Application to Multistage Depressed Collectors for Microwave Amplifiers. NASA TP-1097, 1977.
4. Wintucky, E. G.; Curren, A. N.; and Sovey, J. S.: Electron Reflection and Secondary Emission Characteristics of Sputter-Textured Pyrolytic Graphite Surfaces. Thin Solid Films, vol. 84, 1981, pp. 161-169. (Also NASA TM-81755, 1981.)
5. Curren, A. N.; and Jensen, K. A.: Beam Impingement Angle Effects on Secondary Electron Emission Characteristics of Textured Pyrolytic Graphite, NASA TP-2285, 1984.
6. Curren, A. N.; and Fox, T. A.: Traveling-Wave Tube Efficiency Improvement with Textured Pyrolytic Graphite Multistage Depressed Collector Electrodes. IEEE Electron Device Lett., vol. EDL-2, Oct. 1981, pp. 252-254.
7. Kohl, Walter H.: Handbook of Materials and Techniques for Vacuum Devices. Reinhold, 1967.
8. Semiconductor/Metallurgical Grades. Poco Graphite, Inc., Decatur, Texas, 1978.
9. Wehner, G. K.; and Hajicek, D. J.: Cone Formation on Metal Targets During Sputtering. J. Appl. Phys., vol. 42, no. 3, Mar. 1971, pp. 1145-1149.

1. Report No.	2. Government Accession No.	3. Recipient's Catalog No.
NASA TP-2342		

4. Title and Subtitle	5. Report Date
Secondary Electron Emission Characteristics of Ion-Textured Copper and High-Purity Isotropic Graphite Surfaces	July 1984
	6. Performing Organization Code
7. Author(s)	8. Performing Organization Report No.
Arthur N. Curren and Kenneth A. Jensen	E-2064
	10. Work Unit No.
9. Performing Organization Name and Address	11. Contract or Grant No.
National Aeronautics and Space Administration Lewis Research Center Cleveland, Ohio 44135	13. Type of Report and Period Covered
	Technical Paper
12. Sponsoring Agency Name and Address	14. Sponsoring Agency Code
National Aeronautics and Space Administration Washington, D.C. 20546	

15. Supplementary Notes

16. Abstract

Experimentally determined values of true secondary electron emission and relative values of reflected primary electron yield for untreated and ion-textured oxygen-free high conductivity copper and untreated and ion-textured high-purity isotropic graphite surfaces are presented for a range of primary electron beam energies and beam impingement angles. This investigation was conducted to provide information that would improve the efficiency of multistage depressed collectors (MDC's) for microwave amplifier traveling-wave tubes in space communications and aircraft applications. For high efficiency, MDC electrode surfaces must have low secondary electron emission characteristics. Although copper is a commonly used material for MDC electodes, it exhibits relatively high levels of secondary electron emission if its surface is not treated for emission control. Recent studies have demonstrated that high-purity isotropic graphite is a promising material for MDC electrodes, particularly with ion-textured surfaces. The materials were tested at primary electron beam energies of 200 to 2000 eV and at direct (0°) to near-grazing (85°) beam impingement angles. True secondary electron emission and relative relected primary electron yield characteristics of the ion-textured surfaces were compared with each other and with those of untreated surfaces of the same materials. Both the untreated and ion-textured graphite surfaces and the ion-treated copper surface exhibited sharply reduced secondary electron emission characteristics relative to those of untreated copper. The ion-treated graphite surface yielded the lowest emission levels.

17. Key Words (Suggested by Author(s))	18. Distribution Statement
Secondary electron emission; Graphite, Carbon; Traveling-wave tubes; Multi-stage depressed collector; Copper	Unclassified - unlimited STAR Category 27

19. Security Classif. (of this report)	20. Security Classif. (of this page)	21. No. of pages	22. Price*
Unclassified	Unclassified	15	A02

*For sale by the National Technical Information Service, Springfield, Virginia 22161

NASA-Langley, 1984